Phosphorylation of STIM1 at ERK1/2 target sites modulates store-operated calcium entry

Eulalia Pozo-Guisado[1], David G. Campbell[2], Maria Deak[2], Alberto Álvarez-Barrientos[3], Nicholas A. Morrice[2], Ignacio S. Álvarez[4], Dario R. Alessi[2] and Francisco Javier Martín-Romero[1,*]

[1]Department of Biochemistry and Molecular Biology, College of Life Sciences, University of Extremadura, Badajoz, 06071, Spain
[2]MRC Protein Phosphorylation Unit, College of Life Sciences, University of Dundee, Dow Street, Dundee, DD1 5EH, UK
[3]Bioscience Applied Techniques Facility, University of Extremadura, Badajoz, 06071, Spain
[4]Department of Cell Biology, College of Life Sciences, University of Extremadura, Badajoz, 06071, Spain
*Author for correspondence (fjmartin@unex.es)

Summary

Store-operated calcium entry (SOCE) is an important Ca^{2+} entry pathway that regulates many cell functions. Upon store depletion, STIM1, a transmembrane protein located in the endoplasmic reticulum (ER), aggregates and relocates close to the plasma membrane (PM) where it activates store-operated calcium channels (SOCs). Although STIM1 was early defined as a phosphoprotein, the contribution of the phosphorylation has been elusive. In the present work, STIM1 was found to be a target of extracellular-signal-regulated kinases 1 and 2 (ERK1/2) in vitro, and we have defined the ERK1/2-phosphorylated sites on the STIM1 sequence. Using HEK293 cells stably transfected for the expression of tagged STIM1, we found that alanine substitution mutants of ERK1/2 target sites reduced SOCE significantly, suggesting that phosphorylation of these residues are required to fully accomplish SOCE. Indeed, the ERK1/2 inhibitors PD184352 and PD0325901 decreased SOCE in transfected cells. Conversely, 12-O-tetradecanoylphorbol-13-acetate, which activates ERK1/2, enhanced SOCE in cells expressing wild-type tagged STIM1, but did not potentiate Ca^{2+} influx in cells expressing serine to alanine mutations in ERK1/2 target sites of STIM1. Alanine substitution mutations decreased Ca^{2+} influx without disturbing the aggregation of STIM1 upon store depletion and without affecting the relocalization in ER–PM punctae. However, our results suggest that STIM1 phosphorylation at ERK1/2 target sites can modulate SOCE by altering STIM1 binding to SOCs, because a significant decrease in FRET efficiency was observed between alanine substitution mutants of STIM1–GFP and ORAI1–CFP.

Key words: STIM1, Calcium, Store-operated calcium entry, SOCE, Phosphorylation, ERK1/2

Introduction

STIM1 (stromal interaction molecule 1) protein has been described as a key regulator of store-operated calcium entry (SOCE) (Liou et al., 2005; Roos et al., 2005), one of the most important calcium entry pathways in non-excitable cells. This single-transmembrane protein contains an EF-hand domain close to the N-terminus that acts as a Ca^{2+} sensor within the luminal space of the endoplasmic reticulum (ER). The cytosolic side of STIM1 contains a double coiled-coil, within an ezrin/radixin/moesin (ERM) domain, that has a role in the activation of Ca^{2+} entry through store-operated calcium channels (SOCs) located in the plasma membrane (PM) (for a review, see Cahalan, 2009). Upon depletion of calcium concentration within the ER, the sterile alpha motif (SAM) interaction domain, adjacent to the EF-hand domain, mediates the oligomerization of STIM1 (Liou et al., 2007). This oligomerization leads to the relocalization of STIM1 in puncta-like ER–PM junctions (Liou et al., 2007; Muik et al., 2008; Smyth et al., 2008). STIM1 clustering and relocalization is required for the activation of SOCs. In a variety of cell types, SOCs carry a highly Ca^{2+}-selective, non-voltage-gated, inwardly rectifying current, known as the Ca^{2+} release activated Ca^{2+} current (CRAC). Although the molecular nature of these SOCs remained elusive for a long time, both SOCE and the CRAC current have been found to require the activation of ORAI1 (also known as CRACM1), a PM four-transmembrane spanning protein that constitutes the CRAC channel (Feske et al., 2006; Soboloff et al., 2006; Vig et al., 2006; Zhang

et al., 2006). Although the mechanistic details of SOC activation are still under study, it is accepted that STIM1 multimerization triggers the binding to ORAI1 (Yeromin et al., 2006) to form active channels. In addition, STIM1 couples to transient receptor potential canonical (TRPC) channels, except TRPC7, to regulate their function as SOCs (Yuan et al., 2007). The heteromeric interactions of TRPC1 with other TRPCs can generate SOCs with different properties, and TRPC1 also associates with ORAI1 to produce TRPC1–ORAI1–STIM1 ternary complexes that act as SOCs (Ambudkar et al., 2007).

The C-terminal portion of STIM1 is sufficient for the activation of ORAI1, and the physical coupling of both proteins is mediated by a coiled-coil domain in the N-terminus of ORAI1 (Muik et al., 2008). Some molecular aspects of ORAI1 gating by STIM1 that have been described recently involve a highly conserved CRAC activation domain of STIM1 of about 100 amino acids that binds directly to ORAI1 to open the Ca^{2+} channel. This domain has been denominated CAD (CRAC activation domain) or SOAR (STIM1 ORAI1 activation region) (Park et al., 2009; Yuan et al., 2009). An electrostatic gating mechanism is involved in the case of the TRPCs, because STIM1 gates TRPC1 through the interaction of two negatively charged aspartates in TRPC1 and the conserved polybasic domain close to the C-terminus of STIM1 (Zeng et al., 2008).

STIM1 was early defined as a phosphoprotein (Manji et al., 2000). An in silico search shows that the cytosolic C-terminus

domain contains potential target residues for different kinases, and large-scale mass spectrometry has revealed phosphorylation of serine residues in STIM1 (Olsen et al., 2006). However, the molecular pathway controlling this phosphorylation and the possible function of the phosphorylated residues remain unknown. In the present work, we studied the molecular details of STIM1 phosphorylation in order to determine any upstream kinases that regulate STIM1 function and therefore SOCE activation. We found that STIM1 is a probable target of of extracellular-signal-regulated kinases 1 and 2 (ERK1/2) in asynchronous cultures of HEK293 cells, and that the serine to alanine mutation of target residues reduced STIM1–ORAI1 binding. Our results suggest a mechanism of SOCE modulation that is mediated by STIM1 phosphorylation.

Results
STIM1 is phosphorylated in HEK293 cells
To study whether STIM1 is phosphorylated in vivo in HEK293 cells, we generated a Flip-In T-REx HEK293 cell line for the inducible expression of STIM1–GFP. STIM1–GFP expression was induced under a tetracycline-sensitive promoter (supplementary material Fig. S1), and the recombinant protein showed a location profile that matched well with the endoplasmic reticulum (Fig.

1A). The aggregation of STIM1–GFP induced by thapsigargin revealed that this protein was sensitive to Ca^{2+}-store depletion. In parallel experiments, STIM1–GFP was pulled down from HEK293 cells (Fig. 1B) and the protein was digested with Asp-N protease. The resulting peptides were subjected to liquid chromatography and mass spectrometry (LC-MS) with precursor ion scanning on a Q-Trap mass spectrometer, which enabled us to find a number of phosphorylated peptides within the STIM1 sequence (Fig. 1C). Several of these were not amenable to phosphosite identification, but we could assign three serine residues as phosphosites: Ser519, Ser575 and Ser628. The STIM1 phosphorylation profile as shown by Q-Trap analysis indicated the presence of similar phosphopeptides in both resting cells and cells treated with thapsigargin in Ca^{2+}-free medium (Fig. 1C,D). Moreover, comparison of the peak heights of the two conditions showed that there was no major variation in the phosphorylation level of these peptides under store depletion conditions. With the analysis of phosphopeptides using an LTQ Orbitrap XL mass spectrometer, we could significantly assign two serine residues, Ser519 and Ser575, within all the phosphopeptides detected (Fig. 1D).

Ser575 is within the reported optimal target sequence for ERK1/2 (PXS/TP), suggesting that ERK1/2 could be one of the upstream
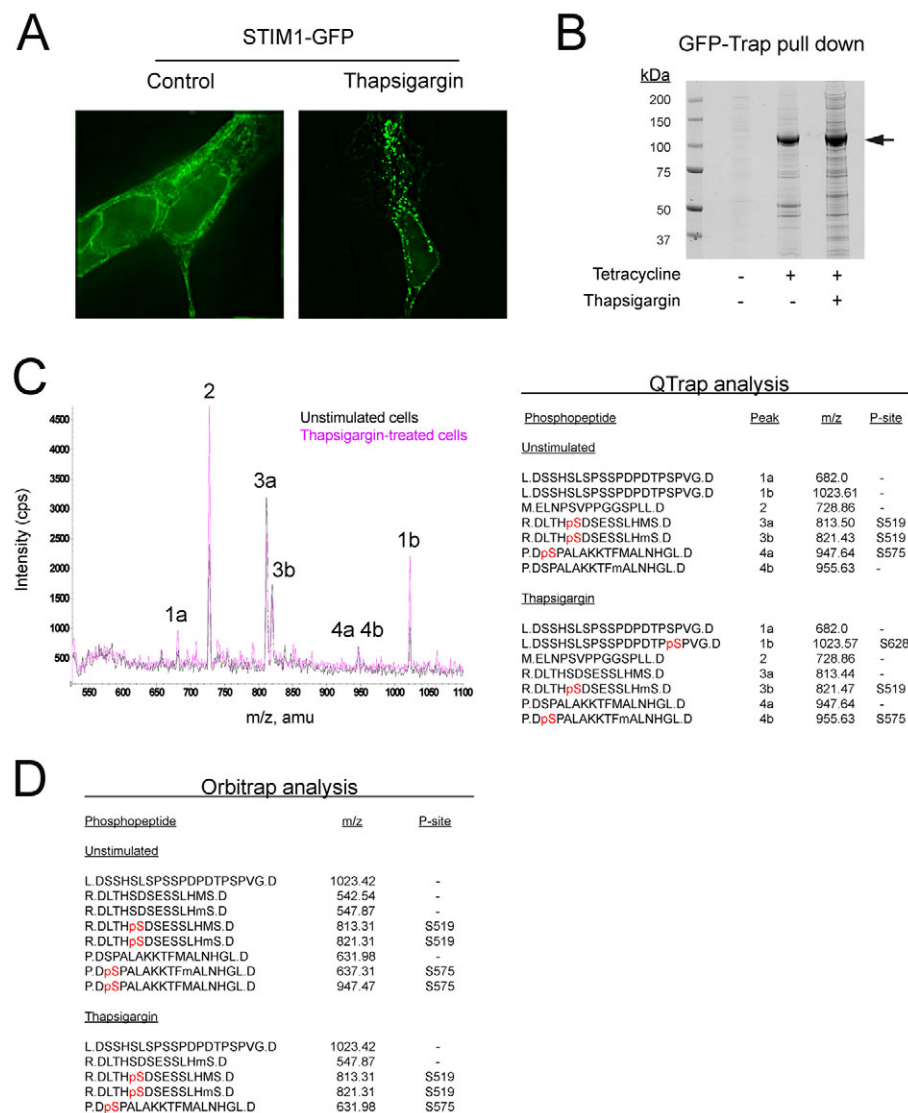

A STIM1-GFP
Control | Thapsigargin

B GFP-Trap pull down

kDa
200
150
100
75
50
37

Tetracycline	-	+	+
Thapsigargin	-	-	+

C

Unstimulated cells
Thapsigargin-treated cells

y-axis: Intensity (cps)
x-axis: m/z, amu

QTrap analysis

Phosphopeptide	Peak	m/z	P-site
Unstimulated			
L.DSSHSLSPSSPDPDTPSPVG.D	1a	682.0	-
L.DSSHSLSPSSPDPDTPSPVG.D	1b	1023.61	-
M.ELNPSVPPGGSPLL.D	2	728.86	-
R.DLTHpSDSESSLHMS.D	3a	813.50	S519
R.DLTHpSDSESSLHmS.D	3b	821.43	S519
P.DpSPALAKKTFMALNHGL.D	4a	947.64	S575
P.DSPALAKKTFmALNHGL.D	4b	955.63	-
Thapsigargin			
L.DSSHSLSPSSPDPDTPSPVG.D	1a	682.0	-
L.DSSHSLSPSSPDPDTPpSPVG.D	1b	1023.57	S628
M.ELNPSVPPGGSPLL.D	2	728.86	-
R.DLTHSDSESSLHMS.D	3a	813.44	-
R.DLTHpSDSESSLHmS.D	3b	821.47	S519
P.DSPALAKKTFMALNHGL.D	4a	947.64	-
P.DpSPALAKKTFmALNHGL.D	4b	955.63	S575

D Orbitrap analysis

Phosphopeptide	m/z	P-site
Unstimulated		
L.DSSHSLSPSSPDPDTPSPVG.D	1023.42	-
R.DLTHSDSESSLHMS.D	542.54	-
R.DLTHSDSESSLHmS.D	547.87	-
R.DLTHpSDSESSLHMS.D	813.31	S519
R.DLTHpSDSESSLHmS.D	821.31	S519
P.DSPALAKKTFMALNHGL.D	631.98	-
P.DpSPALAKKTFmALNHGL.D	637.31	S575
P.DpSPALAKKTFMALNHGL.D	947.47	S575
Thapsigargin		
L.DSSHSLSPSSPDPDTPSPVG.D	1023.42	-
R.DLTHSDSESSLHmS.D	547.87	-
R.DLTHpSDSESSLHMS.D	813.31	S519
R.DLTHpSDSESSLHmS.D	821.31	S519
P.DpSPALAKKTFMALNHGL.D	631.98	S575

Fig. 1. Mapping of in vivo STIM1 phosphorylation sites. (**A**) HEK293 Flip-In T-REx cells expressing STIM1–GFP were incubated in HBSS as a control (left) or in Ca^{2+}-free HBSS with 1 μM thapsigargin for 10 minutes (right) and visualized under wide-field fluorescence microscopy in order to evaluate STIM1 multimerization under store-depletion conditions. (**B**) HEK293 Flip-In T-REx cells were incubated under the experimental conditions described for A, and expressed STIM1–GFP was pulled-down with GFP binder. STIM1–GFP (labeled by the arrow) was excised from a colloidal Coomassie-Blue-stained polyacrylamide gel, and digested with Asp-N protease. (**C**) One-tenth of the digest was subjected to LC-MS with precursor ion scanning and the phosphorylated residues were identified by inspection of the acquired MSMS spectra (left) as described in Materials and Methods. The y-axis denotes the ion intensity of the −79 ±1 ions [$PO_3^{(-)}$] in counts per second (cps), and the x-axis the mass:charge ratio. Here and in Fig. 1D the identified phosphopeptides are listed with phosphorylated residues (where identifiable) denoted in red (pS, for phosphoserine), and methionine sulfoxide residues denoted by m. The m/z values are for the positive ions fragmented during MSMS analysis. (**D**) One-tenth of the digest was subjected to LC-MS on a Thermo-Electron LTQ-Orbitrap mass spectrometer. Other experimental conditions as in C.

kinases that phosphorylates STIM1 in HEK293 cells. To evaluate the involvement of ERK1/2 in this phosphorylation, we treated cells expressing STIM1–GFP with 12-*O*-tetradecanoylphorbol-13-acetate (TPA), a well known activator of the ERK1/2 pathway. The pulled-down protein was analyzed as described above, and the combined Q-Trap and Orbitrap analysis yielded the same list of phosphopeptides as described for the treatment with thapsigargin (Fig. 2). It is noteworthy that other residues can probably be phosphorylated in resting, or thapsigargin- or TPA-treated cells, because we found phosphopeptides with assignment scores outside the significance level (i.e. $P>0.05$). Thus, our results did not exclude the possibility that other phosphoaminoacids might be found in the STIM1 sequence in addition to Ser519, Ser575 and Ser628.

ERK1/2 phosphorylates GST–STIM1 in vitro

To look further into our initial findings, we cloned the cytosolic domain of STIM1 (STIM1[235-END]) into a PGEX-6-P1 plasmid and purified GST–STIM1[235-END] from BL21 *Escherichia coli* cells. Because Ser575 was a plausible target of ERK1/2 activity, the purified GST–STIM1[235-END] protein was used as the substrate in an in vitro kinase assay with both ERK1 and ERK2 in the presence of Mg-$[\gamma^{32}P]$ATP. The results shown in Fig. 3A indicate that ERK1 and ERK2 effectively phosphorylated the cytosolic domain of STIM1 in vitro. Subsequent LC-MS analysis of the trypsin-digested phosphorylated substrate on a Q-Trap mass spectrometer indicated that Ser575 was phosphorylated in our in vitro kinase assay in the presence of ERK1 (Fig. 3C–E) and ERK2 (Fig. 3E). Because trypsin-digested protein yielded, from within the S/P domain of STIM1, peptides too short for MS analysis, a second set of samples was digested with Asp-N protease and analyzed as described for trypsin digestion. With a lower signal-to-background ratio, we could assign Ser575 to the phosphoresidue in some of the ions shown in Fig. 3D. Although this assignment was below the significant score when the assay was performed with ERK1 (Fig. 3E) in Asp-N digested samples, a parallel assay with ERK2 had a significant score that let us assign the phosphosite of the peptide

P.DSPALAKKTFMALNHGL.D to Ser575. Other major ions were found in the Asp-N digested samples (numbered 1–5 in Fig. 3D,E) despite the fact that the identity of the phosphosites was outside the statistical significance level ($P>0.05$). It is worth mentioning that some of these potential phosphosites in the in vitro kinase assay, such as Ser608 and Ser621, were within the optimal reported sequence for ERK1/2, suggesting that these sites could be targets of ERK1/2 in vivo as well. In addition, Ser608 and Ser621 were found in the sequences of the phosphopeptides detected in our QTrap analysis in vivo (see Fig. 1C), although the assignment of Ser608 and Ser621 as phosphoaminoacids could not be demonstrated in vivo with statistical confidence.

The possibility that additional amino acids in the STIM1 sequence can be phosphorylated by ERK1/2 was studied by mutating Ser575, Ser608, and Ser621 to alanine (S575A, S608A, S621A), allowing us to evaluate by autoradiography whether incorporation of ^{32}P occurred after an in vitro kinase assay using the mutated GST–STIM1[235-END] purified from *E. coli* as substrate. It is shown in Fig. 3F that the phosphorylation signal was depleted to background levels when GST–STIM1[235-END (S575A/S608A/S621A)] was used, demonstrating that no other residues were phosphorylated in the cytosolic domain of STIM1 by ERK1/2 in vitro. In addition, when single mutants S575A, S608A or S621A were used as substrates, phosphorylation signal was significantly reduced (supplementary material Fig. S2), indicating that Ser575, Ser608 and Ser621 are phosphorylated in vitro by ERK1/2 and contribute to STIM1 phosphorylation. These three residues were found within different phosphopeptides in HEK293 cells, either in resting conditions, or in thapsigargin- or TPA-treated cells (Fig. 1C and Fig. 2A), amongst other phosphoaminoacids, suggesting that ERK1/2 (in addition to other unspecified kinases) phosphorylates STIM1 in vivo.

Phosphorylation of STIM1 at ERK1/2 target sites is required to activate SOCE

The functional consequences of the phosphorylation of STIM1 at ERK1/2 target sites were studied using HEK293 cells with stable
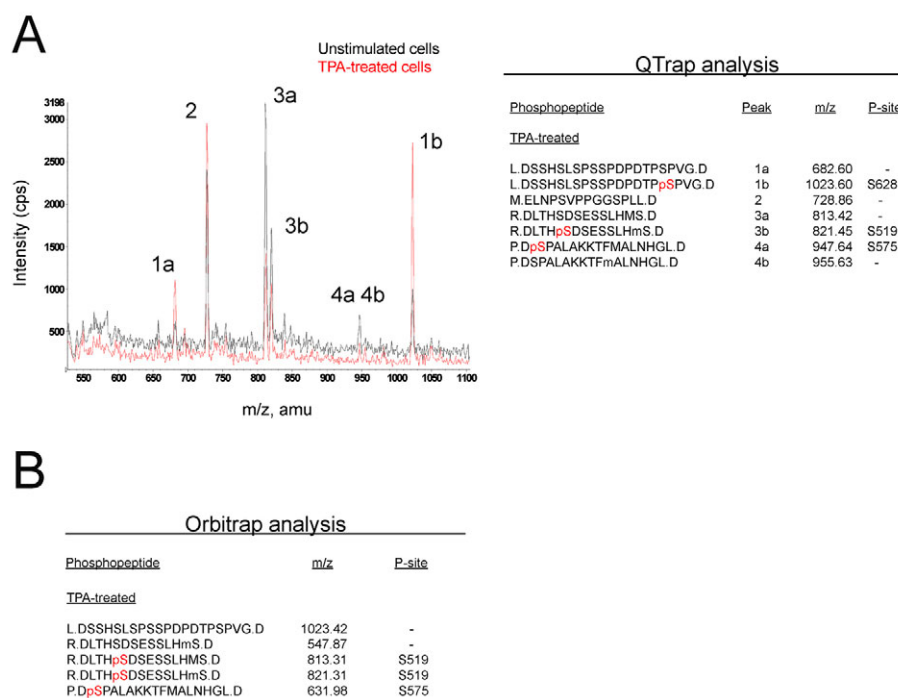
QTrap analysis

Phosphopeptide	Peak	m/z	P-site
TPA-treated			
L.DSSHSLSPSSPDPDTPSPVG.D	1a	682.60	-
L.DSSHSLSPSSPDPDTPpSPVG.D	1b	1023.60	S628
M.ELNPSVPPGGSPLL.D	2	728.86	-
R.DLTHSDSESSLHMS.D	3a	813.42	-
R.DLTHpSDSESSLHmS.D	3b	821.45	S519
P.DpSPALAKKTFMALNHGL.D	4a	947.64	S575
P.DSPALAKKTFmALNHGL.D	4b	955.63	-

Orbitrap analysis

Phosphopeptide	m/z	P-site
TPA-treated		
L.DSSHSLSPSSPDPDTPSPVG.D	1023.42	-
R.DLTHSDSESSLHmS.D	547.87	-
R.DLTHpSDSESSLHMS.D	813.31	S519
R.DLTHpSDSESSLHmS.D	821.31	S519
P.DpSPALAKKTFMALNHGL.D	631.98	S575

Fig. 2. Mapping of in vivo STIM1 phosphorylation sites after treatment with TPA. HEK293 Flip-In T-REx cells expressing STIM1–GFP were incubated in HBSS (unstimulated cells) or in Ca^{2+}-containing medium with 400 ng/ml TPA for 15 minutes (TPA-treated cells). STIM1–GFP was pulled-down with GFP binder, excised from a colloidal Coomassie-Blue-stained polyacrylamide gel, and digested with Asp-N protease. **(A)** One-tenth of the digest was subjected to LC-MS with precursor ion scanning, as described for Fig. 1. Phosphorylated residues were identified by inspection of the acquired MS/MS spectra (left) as described in Materials and Methods. Here and in Fig. 2B the identified peptides are listed with phosphorylated residues (where identifiable) denoted in red (pS, for phosphoserine), and methionine sulfoxide residues denoted by m. The m/z values are for the positive ions fragmented during MS/MS analysis. **(B)** One-tenth of the digest was subjected to LC-MS on a Thermo-Electron LTQ-Orbitrap mass spectrometer, and identified phosphopeptides are listed. Other experimental conditions as in Fig. 1.
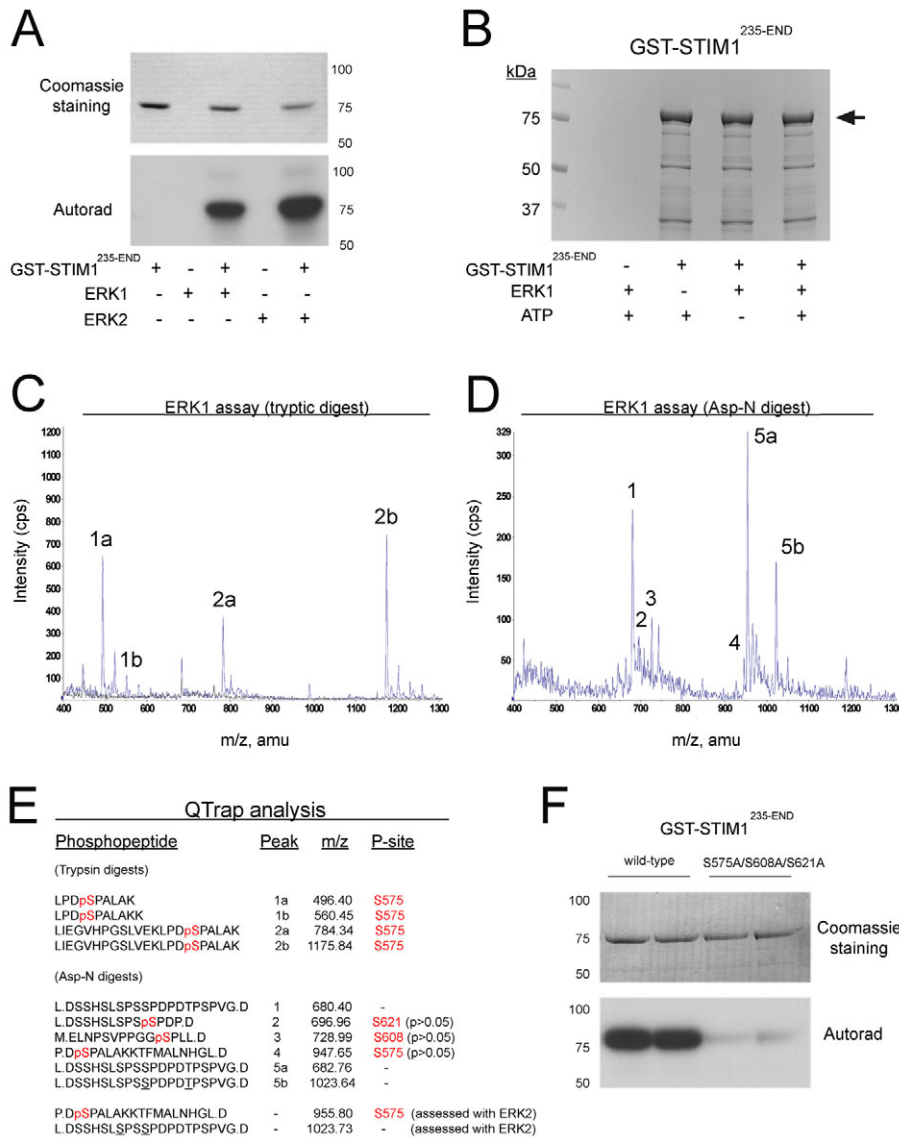
Fig. 3. Identification of residues on STIM1 that are phosphorylated by ERK1/2 in vitro. (A) *E. coli*-expressed GST–STIM1[235-END] was incubated with the indicated active forms of ERK in the presence of Mg[γ^{32}P]ATP for 15 minutes. Phosphorylation of GST–STIM1[235-END] was determined following electrophoresis and subsequent autoradiography of the Coomassie-Blue-stained bands corresponding to GST–STIM1[235-END]. **(B)** Purified GST–STIM1[235-END] was incubated with ERK1 in the presence or absence of Mg-ATP for 15 minutes. GST–STIM1[235-END] was excised from a colloidal Coomassie-Blue-stained polyacrylamide gel and digested with trypsin or Asp-N protease. One-tenth of the trypsin digest **(C)** or the Asp-N digest **(D)** was subjected to LC-MS with precursor ion scanning, and the phosphorylated residues were identified by inspection of the acquired MSMS spectra. **(E)** The identified peptides are listed with phosphorylated residues denoted in red (pS, for phosphoserine), and methionine sulfoxide residues denoted by m. The m/z values are for the positive ions fragmented during MS/MS analysis. In addition, two phosphopeptides obtained after proteolysis of samples assessed with ERK2 are shown in this list (other experimental conditions as described for the assay with ERK1). Phosphopeptides identified with non-significant scores are labeled with $P>0.05$. **(F)** *E. coli*-expressed GST–STIM1[235-END] and the alanine substitution mutant GST–STIM1[235-END (S575A/S608A/S621A)] were incubated with the active form of ERK1 in the presence of Mg[γ^{32}P]ATP for 15 minutes. Phosphorylation of GST–STIM1[235-END] and GST–STIM1[235-END (S575A/S608A/S621A)] was determined following electrophoresis and subsequent autoradiography of the Coomassie-Blue-stained bands corresponding to these substrates.

and inducible expression of STIM1–GFP and FLAG–STIM1. Firstly, SOCE was measured in cells expressing FLAG–STIM1 (Fig. 4A) using a standard protocol with thapsigargin in Ca^{2+}-free medium to induce the emptying of the ER. The transient peak of the ratio F340:F380 just after addition of thapsigargin denoted that the release of Ca^{2+} from the ER in HEK293 cells expressing FLAG–STIM1 was similar to that found in HEK293 cells without overexpression of FLAG–STIM1 (i.e. cells with expression of endogenous STIM1 only). However, subsequent Ca^{2+} entry after store-depletion was enhanced by the stable overexpression of FLAG–STIM1. The expression of FLAG–STIM1 over the endogenous STIM1 levels can be calculated from the immunoblots shown in Fig. 4B. The estimated ratio of FLAG–STIM1 to endogenous STIM1 ranged from 10:1 to 12:1. The fact that the overexpression of FLAG–STIM1 did not induce a 10- to 12-fold increase of SOCE can be rationalized in terms of a limited amount of SOCs responsible for Ca^{2+} entry. In parallel, we developed a cell line with an inducible and stable expression of a mutant variant of FLAG–STIM1, in which those serine residues phosphorylated in vitro by ERK1/2 were mutated to alanine in order to abrogate phosphorylation of STIM1 by ERK1/2 in vivo. However, the

expression of FLAG–STIM1[S575A/S608A/S621A] did not enhance SOCE over the endogenous levels in HEK293 cells (Fig. 4A), with the ratio of tagged protein to endogenous STIM1 in this cell line being similar to that calculated for the wild-type FLAG–STIM1 described above (i.e. 10:1 to 12:1). These results suggest that STIM1, dephosphorylated at ERK1/2 target sites, cannot trigger Ca^{2+} entry (Fig. 4C). This conclusion was further supported by the fact that the treatment of cells with ATP and carbachol induced a transient peak in the $[Ca^{2+}]_i$ that was similar for cells expressing either FLAG–STIM1 or FLAG–STIM1[S575A/S608A/S621A], indicating a similar Ca^{2+} release from the ER in response to P2Y and cholinergic receptor stimulation. However, the subsequent Ca^{2+} influx was significantly reduced in cells expressing FLAG–STIM1[S575A/S608A/S621A] (Fig. 4D), which demonstrated the lack of functional response of SOCs when STIM1 is constitutively dephosphorylated at ERK1/2 target sites. This result is of particular interest because it highlights the modulation of SOCE by STIM1 phosphorylation, probably mediated by ERK1/2, in HEK293 cells.

Because ERK1/2 is a probable upstream kinase for STIM1 in vivo, we studied further the involvement of this kinase in SOCE regulation. Treatment with thapsigargin led to activation of ERK1/2
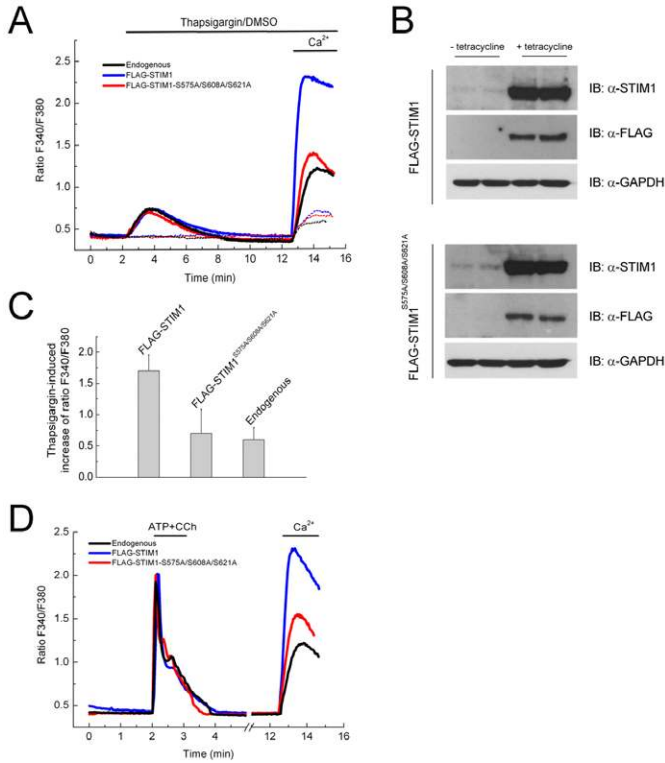
Fig. 4. SOCE in HEK293 cells expressing wild-type and alanine substitution mutant forms of FLAG–STIM1. (A) Cell cultures were treated with 1 µg/ml tetracycline in serum-free DMEM for 12–16 hours (blue and red lines) or left without tetracycline treatment, i.e. with endogenous STIM1 expression only (black lines). The assay to evaluate SOCE in fura-2-loaded cells was performed after addition of 1 µM thapsigargin (solid lines) or the vehicle (DMSO, dashed lines) in Ca^{2+}-free HBSS followed by the addition of 2 mM Ca^{2+}. Ratio F340:F380 was monitored by epifluorescence as indicated in Materials and Methods. (B) Cultures used for the previous assay were evaluated for the wild-type and mutant forms of FLAG–STIM1 expression level by immunoblot using rabbit polyclonal anti-STIM1 or mouse monoclonal anti-FLAG antibodies. Negative controls for FLAG–STIM1 and FLAG–STIM1[S575A/S608A/S621A] expression were performed with the absence of tetracycline treatment, as indicated above. In these latter cultures only endogenous STIM1 was detected without detectable FLAG–peptide expression. The ratio of FLAG–STIM1 to endogenous STIM1 was calculated by volumetric integration of positive bands after subtraction of the background signal. Then, the lower fraction of the membrane was stripped and assessed for the expression of GAPDH as loading control, using a monoclonal anti-GAPDH antibody. (C) The increase of the ratio F340:F380 after Ca^{2+} addition in thapsigargin-treated cells over the increase observed in the absence of thapsigargin was calculated for six independent experiments (20–25 cells per experiment) in endogenous: cultures without tetracycline treatment, in serum-free medium for 12–16 hours, and in FLAG–STIM1 or FLAG–STIM1[S575A/S608A/S621A]: cultures with 1 µg/ml tetracycline in serum-free DMEM for 12–16 hours. (D) SOCE was assessed in fura-2-loaded cells after addition of 100 µM ATP plus 100 µM carbachol (ATP+CCh) in Ca^{2+}-free medium as indicated above. Traces are representative of three independent experiments (20–25 cells per experiment).

(Fig. 5A), sustaining the hypothesis of the involvement of ERK1/2 as upstream kinase of STIM1. Under the same experimental conditions, i.e. after 10 minutes of treatment with 1 µM thapsigargin, an increase in the phosphorylation level of immunoprecipitated FLAG–STIM1 was observed (Fig. 5B). This thapsigargin-stimulated phosphorylation was monitored with an anti-phospho-MAPK/CDK substrate antibody, which recognizes
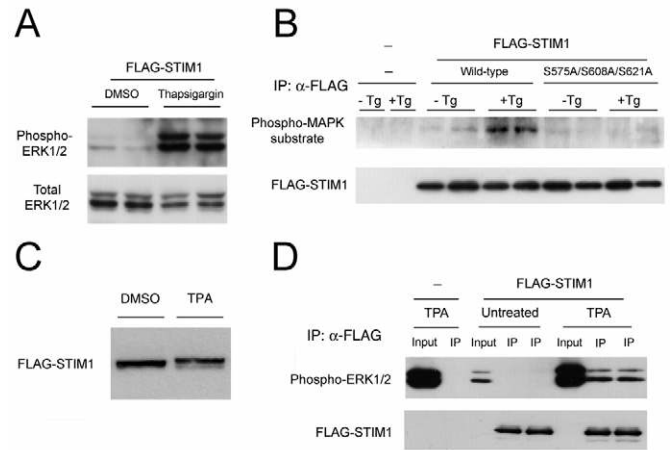

Fig. 5. Activation of ERK1/2 by thapsigargin or TPA, and consequences on STIM1 phosphorylation. Cell cultures were treated with 1 µg/ml tetracycline in serum-free DMEM for 12–16 hours to induce the overexpression of FLAG–STIM1. (A) Then, cells were incubated with 1 µM thapsigargin (or with the vehicle, DMSO) in Ca^{2+}-free medium for 10 minutes, and lysates were assessed for the level of phospho-ERK1/2 and total ERK1/2 by immunoblot as described in Materials and Methods. (B) Cells expressing FLAG–STIM1 or FLAG–STIM1[S575A/S608A/S621A] were incubated in Ca^{2+}-free medium (–Tg) or in Ca^{2+}-free medium plus 1 µM Tg (+Tg) for 10 minutes, and tagged STIM1 was immunoprecipitated with FLAG–agarose beads. Eluted protein from the beads (IP) was electrophoresed and immunoblotted with an anti-phospho-MAPK/CDK substrate (PXpSP or pSPXR/K) antibody. The membrane was stripped and assessed for the expression of FLAG–protein as loading control, using a monoclonal anti-FLAG antibody. (C) Cells expressing FLAG–STIM1 were treated with 400 ng/ml TPA for 15 minutes or with the vehicle (DMSO), and lysates (5 µg) were electrophoresed and immunoblotted with the monoclonal anti-FLAG antibody in order to analyze the band-shift produced by the treatment with TPA. (D) FLAG–STIM1 was immunoprecipitated from 400 ng/ml TPA-treated or untreated cells with FLAG–agarose beads. Eluted protein from the beads (IP) was electrophoresed and immunoblotted for phospho-ERK1/2. In addition, 5 µg of total lysates was added to this experiment (input) in order to evaluate ERK1/2 activation after TPA treatment (compare input from untreated and TPA-treated cells). The upper fraction of the membrane was assessed for the expression of FLAG–peptide as loading control, using a monoclonal anti-FLAG antibody.

phospho-serine in a PXSP or SPXR/K motif. By contrast, FLAG–STIM1[S575A/S608A/S621A] did not show the thapsigargin-stimulated increase of phosphorylation, demonstrating that these sites are phosphorylated in vivo during the treatment with thapsigargin, and further supporting a role for phosphorylated Ser575, Ser608, and Ser621 in the modulation of SOCE.

On the other hand, MEK1 and MEK2 activate p44 and p42 MAPK (ERK1/2) through phosphorylation of activation T-loop residues Thr202/Tyr204 and Thr185/Tyr187, respectively (Rubinfeld and Seger, 2005), and the treatment with phorbol esters is another stimulus that activates the RAF–MEK–ERK kinase pathway. We treated HEK293 cells expressing FLAG–STIM1 with TPA in Ca^{2+}-containing medium. In these conditions, STIM1 from TPA-treated cells showed a band-shift in SDS-PAGE (Fig. 5C), similar to that reported for many other phosphorylated proteins. In addition, phospho-ERK1/2 co-immunoprecipitated with FLAG–STIM1 from HEK293 cells under TPA treatment to a larger extent than when immunoprecipitated from untreated cells (Fig. 5D).

Although the MS results shown above revealed minor variances in the level of phosphorylation between resting and thapsigargin- or
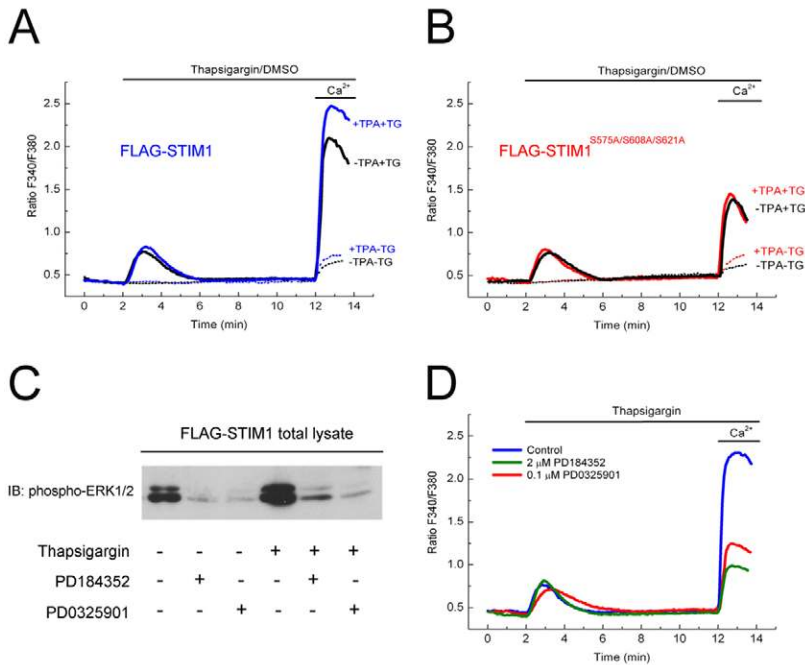
Fig. 6. Inactivation of ERK1/2 by MEK1/2 inhibitors, or activation by TPA, modulated SOCE in cells expressing FLAG–STIM1. Cell cultures were treated with 1 μg/ml tetracycline in serum-free DMEM for 12–16 hours to induce the overexpression of FLAG–STIM1. (**A**) TPA (400 ng/ml) was added to fura-2-loaded cells in Ca^{2+}-free HBSS 3 minutes prior to the beginning of the SOCE assay (blue lines). Thapsigargin (1 μM, solid line) or the vehicle (DMSO, dashed line) was added, and 10 minutes later 2 mM Ca^{2+} was added to the extracellular medium. The total incubation time with TPA was 15 minutes. Parallel controls were performed in the absence of TPA treatment (black lines). The ratio F340:F380 was monitored by epifluorescence microscopy. (**B**) Experimental conditions as for A, using cell cultures expressing FLAG–STIM1[S575A/S608A/S621A]. Red lines correspond to TPA-treated cells and black lines to untreated cells. (**C**) Cells expressing FLAG–STIM1 were incubated with 1 μM thapsigargin (or with the vehicle, DMSO) in Ca^{2+}-free medium for 10 minutes. Prior to the addition of thapsigargin, 2 μM PD184352 or 0.1 μM PD0325901 were added to the Ca^{2+}-free medium. Lysates from these cultures were assessed for the level of phospho-ERK1/2 by immunoblot as described in Materials and Methods. (**D**) Following a similar experimental procedure, i.e. addition of the inhibitors PD184352 or PD0325901 5 minutes prior to the addition of thapsigargin in Ca^{2+}-free medium, SOCE was evaluated in cells expressing FLAG–STIM1 after addition of 1 μM thapsigargin.

TPA-treated cells, Q-Trap analysis is not an adequate method for the determination of the level of phosphorylation. However, using this method we found the same list of phosphopeptides in resting, thapsigargin- or TPA-treated cells. This result, together with: (1) the increased level of phosphorylation in STIM1 during the treatment with thapsigargin, which is prevented by serine to alanine substitution mutants, (2) the increased phospho-ERK1/2 co-immunoprecipitation, and (3) the electrophoretic retardation of STIM1 from TPA-treated cells, leads to the conclusion that the thapsigargin and TPA treatments do not increase the number of phosphosites in the STIM1 sequence, but increase the pool of phosphorylated STIM1.

Coherent with the hypothesis that STIM1 is a substrate of ERK1/2 and that this phosphorylation is required to activate SOCE, we found that TPA enhanced the thapsigargin-triggered SOCE in cells expressing FLAG–STIM1 (Fig. 6A). However, TPA did not modify the extent of SOCE in FLAG–STIM[S575A/S608A/S621A] cells (Fig. 6B), strongly supporting the idea that ERK1/2 activation is ruling the phosphorylation of STIM1 and that phosphorylation of these residues is required for the accomplishment of thapsigargin-induced SOCE in HEK293 cells.

The results of the use of specific inhibitors of ERK1/2 to further test our conclusions should be considered with caution, because these kinds of experiments do not discriminate the diverse targets of ERK1/2, and it is possible that ERK1/2 might phosphorylate other components in the molecular machinery governing SOCE, including microtubules and calcium channels. We used PD0184352 and PD0325901 as specific inhibitors of the activation of ERK1/2 (Bain et al., 2007) and assessed SOCE following the standard protocol with the addition of thapsigargin and Ca^{2+} to the medium. Both inhibitors, at concentrations that fully inhibited the activation of ERK1/2 (Fig. 6C), induced a strong inhibition of SOCE in HEK293 cells triggered by thapsigargin in Ca^{2+}-free medium (Fig. 6D).

S575A/S608A/S621A mutations in STIM1 reduce the binding to ORAI1

The mechanism by which dephosphorylated STIM1 did not fully activate SOCE in response to store depletion was studied further.

STIM1–GFP[S575A/S608A/S621A] did not reveal any significant modification of its location in HEK293 cells when compared to wild-type STIM1–GFP (Fig. 7A), which indicates that phosphorylation by ERK1/2 is not a requirement for the aggregation induced by store depletion. In addition, the relocalization of STIM1–GFP in puncta-like ER–PM junctions (required to activate SOCs) was unaltered by the mutations of the three residues targeted by ERK1/2, because STIM1–GFP[S575A/S608A/S621A] was found to move towards the PM with the same kinetics as the wild-type STIM1–GFP (Fig. 7B). This latter set of results rules out the possibility that the phosphorylation at Ser575, Ser608 and Ser621 sites could be essential for the multimerization of STIM1 or for the relocalization of this protein close to the PM. However, analysis of the fluorescence resonance energy transfer (FRET) in PM areas between stably expressed STIM1–GFP and transiently expressed ORAI1–CFP in these cells indicated that a significant decrease of STIM1–ORAI1 binding was found when STIM1 was constitutively dephosphorylated at the aforementioned residues (Fig. 7C). This conclusion was further confirmed by the study of the level of endogenous ORAI1 that co-immunoprecipitated with FLAG–STIM1. In addition to the expected increase in co-immunoprecipitated ORAI1 after thapsigargin-store depletion in cells expressing FLAG–STIM1, we did not observed this increase in ORAI1 levels when FLAG–STIM1[S575A/S608A/S621A] was immunoprecipitated from thapsigargin-treated HEK293 cells (Fig. 7D). This lower binding explains the level of SOCE observed in alanine substitution mutants in response to store depletion, and suggests a role for the ERK1/2 target sites in SOCE regulation.

Discussion
The present results constitute the first demonstration of the requirement of the phosphorylation of STIM1 at ERK1/2 target sites for the activation of SOCE. Although STIM1 was early defined as a phosphoprotein (Manji et al., 2000), and phosphoproteomic large-scale analysis revealed several phosphorylated residues in STIM1 in HeLa cells treated with epidermal growth factor (Olsen et al., 2006), the physiological
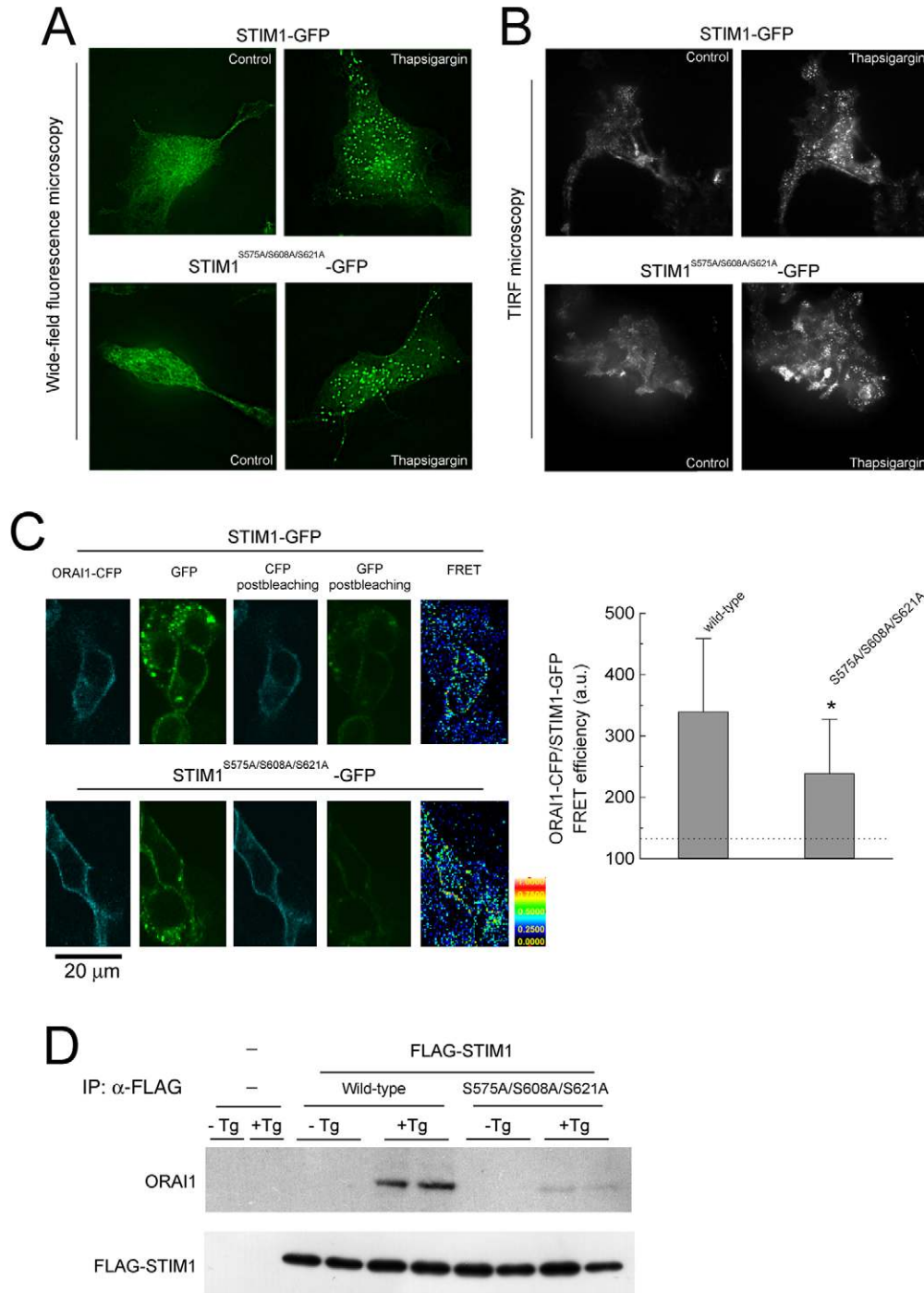
Fig. 7. S575A/S608A/S621A mutations did not alter thapsigargin-induced aggregation or relocalization of STIM1 but decreased the binding to ORAI1. (A) HEK293 Flip-In T-REx cells expressing STIM1–GFP or STIM1[S575A/S608A/S621A]–GFP were incubated in Ca^{2+}-free HBSS (left) or in Ca^{2+}-free HBSS with 1 μM thapsigargin (right). Ten minutes after addition of thapsigargin, cells were fixed with paraformaldehyde and visualized under wide-field fluorescence microscopy. (B) Both cell lines, STIM1–GFP and STIM1[S575A/S608A/S621A]–GFP, were incubated in Ca^{2+}-free HBSS and studied under TIRF microscopy recorded in live-cell imaging (control, left panels). Thapsigargin (1 μM) was added and images taken after 5 minutes (thapsigargin, right panels). GFP fluorescence was monitored under the same microscopy settings throughout the experiment. (C) Cells expressing STIM1–GFP or STIM1[S575A/S608A/S621A]–GFP were transfected for the transient expression of ORAI1–CFP. Cells were incubated in Ca^{2+}-free HBSS with 1 μM thapsigargin for 10 minutes and analyzed for FRET quantification. For FRET quantification purposes, only plasma membrane areas were analyzed. At least 45 cells were measured in each experimental condition. FRET efficiency is expressed in arbitrary units. The dashed line shows the basal fluorescence transfer in the absence of thapsigargin. Two-tailed significance *P<0.001. (D) Cells expressing FLAG–STIM1 or FLAG–STIM1[S575A/S608A/S621A] were incubated in Ca^{2+}-free medium (–Tg) or in Ca^{2+}-free medium plus 1 μM Tg (+Tg) for 10 minutes. Immunoprecipitated FLAG–protein (IP) was assessed with an anti-ORAI1 antibody. The upper fraction of the membrane was excised and assessed for the expression of FLAG–protein as loading control.

implications of this phosphorylation for STIM1 function remained elusive.

Recently, it has been shown that phosphorylation of STIM1 in nocodazole-arrested mitotic HEK293 cells might underlie the suppression of SOCE during mitosis (Smyth et al., 2009). Those authors observed that Ser668 is a target residue of CDK1 activity in vitro and in vivo, but that the truncated form of STIM1, ending at residue 570 to avoid phosphorylation at Ser668 in vivo, failed to support SOCE or to show puncta formation associated with the PM. Nevertheless, the underlying role of phosphorylation at both Ser486 and Ser668 in the suppression of SOCE during mitosis was supported by their finding that mitotic HEK293 cells co-expressing ORAI1 and eYFP–STIM1[S486A/S668A] showed significant increase in SOCE when compared to cells expressing wild-type eYFP–STIM1 (Smyth et al., 2009). Interestingly, those authors found peptides with phosphorylated Ser575, Ser608 and Ser621, amongst other serine residues (Ser492, Ser553, Ser602, Ser620 and Ser668). The serine residues that we have defined in this work as ERK1/2 target residues (i.e. Ser575, Ser608 and Ser 621) were not studied by those authors because they were found to be constitutive (for Ser575 and Ser621) or to undergo dephosphorylation, depending on the cell cycle phase (for Ser608), and their implication in the

STIM1 function was not described. In parallel, Yu and co-workers found several phosphorylated serine and threonine residues in the STIM1 sequence from *Xenopus* oocytes, including Ser575 and Ser621 (Yu et al., 2009). However, their study was restricted to Ser621 in oocytes arrested in meiosis because this residue was the only one consistently found in MS-LC analysis from different batches of samples. SOCE is inactivated in *Xenopus* oocytes arrested in meiosis, as well as during mitosis in HEK293 cells, but Yu et al. found that phosphomimetic or alanine substitution mutants of STIM1 displayed a similar profile of clustering during meiosis of oocytes as compared with wild-type STIM1. Those data ruled out a direct mediation of STIM1 phosphorylation at Ser621 in the inactivation of SOCE during meiosis (Yu et al., 2009).

Our finding that STIM1 requires specific phosphorylation to activate SOCE is therefore a new observation that is not incoherent with those two recent reports focused on the mitotic or meiotic suppression of SOCE. On the contrary, our results are indicative of a requirement of STIM1 phosphorylation at ERK1/2 target residues to achieve activation of SOCE triggered by store depletion. Whether phosphorylation of other residues of STIM1 could be modulating SOCE during mitosis and/or during interphase is beyond the scope of this work. We cannot argue that a dynamic phosphorylation and dephosphorylation of other residues of STIM1 might underlie the inhibition of SOCE during mitosis or meiosis. In our study, MS analysis revealed several residues phosphorylated by ERK1/2 in vitro. It has been described that U0126, an inhibitor of MEK1/2, the upstream kinase of ERK1/2, reduces Ca^{2+} entry stimulated by thapsigargin in platelets (Rosado and Sage, 2001). This therefore suggested the implication of the ERK pathway in SOCE activation, although there was no direct evidence of the possible targets of ERK1/2 during the activation of SOCE in platelets in those initial studies. Other kinase inhibitors have been shown to have a partial effect on Ca^{2+} entry. ML-9, an inhibitor of the myosin light-chain kinase (MLCK), inhibits constitutive SOCE in HEK293 cells expressing EYFP–STIM1$^{D76N/D78N}$ (Smyth et al., 2007), a constitutively active STIM1 mutant. However, those authors argued that the effects of ML-9 on SOCE were not due to inhibition of MLCK, and the molecular target of the effect of ML-9 remained unknown.

We have now found target sites for ERK1/2 activity in the STIM1 sequence, and substitution mutation experiments revealed that no other residues than Ser575, Ser608 and Ser621 were phosphorylated by ERK1/2. Although other kinases are most probably involved in STIM1 regulation, we focused our study on ERK1/2. Our results offer a solid explanation for the early observations using ERK1/2 inhibitors (Rosado and Sage, 2001). The mutation of Ser575, Ser608 and Ser621 to alanine to prevent phosphorylation strongly reduced Ca^{2+} entry. Consequently, inhibitors of MEK1/2 that prevent activation of ERK1/2 reduced Ca^{2+} entry because STIM1 phosphorylation by ERK1/2 is required to activate SOCE. By contrast, TPA, which strongly activates ERK1/2, enhanced SOCE in FLAG–STIM1 cells but not in FLAG–STIM1$^{S575A/S608A/S621A}$. Taken together, our results indicate that, in addition to store depletion, phosphorylation of STIM1 in ERK1/2 sites modulates SOCE. The decrease of SOCE in cells expressing the alanine substitution mutants of STIM1 was observed without disturbing STIM1–GFP$^{S575A/S608A/S621A}$ multimerization in response to store depletion, or the formation of ER–PM junctions. However, FRET and co-immunoprecipitation experiments showed a lower binding of STIM1 to ORAI1, and this observation fully explains the reduced SOCE observed after store depletion.

In conclusion, our results demonstrate the requirement of the phosphorylation of STIM1 in ERK1/2 target serine residues to fully accomplish SOCE triggered by thapsigargin. However, the molecular events triggered by the phosphorylation of these residues that lead to a diminished binding to SOCs are still unclear. It is known that the STIM1 C-terminal domain associates in vitro and in vivo with ORAI1 to stimulate channel function without ORAI1–STIM1 cluster formation (Muik et al., 2008). STIM1 gates TRPC1 by intermolecular electrostatic interaction, although ORAI1 gating by STIM1 does not require the polybasic and Ser/Pro domains (Zeng et al., 2008). The gating of SOCs by STIM1 could be a mechanism modulated by phosphorylation of STIM1. The phosphorylated serine residues described in this work are close to the polybasic lysine-rich domain of STIM1 involved in SOC gating, and the accumulation of negative charges by serine phosphorylation in the Ser/Pro domain could be modulating the gating of SOCs. Nevertheless, the lower binding of dephosphorylated STIM1 to ORAI1 suggests that the phosphorylation of STIM1 could modulate the function of other components required for the binding and the gating of SOCs. In this sense, the number of participants in the activation of SOCs is still increasing and an EF-hand protein, CRACR2A, that binds to ORAI1 upon store depletion and regulates SOCE has been described recently (Srikanth et al., 2010). The possibility that members of the SOCE complex involved in the gating of SOCs could be sensing specific phosphosites in the STIM1 sequence to activate SOCs, is a hypothesis that requires further investigation.

Materials and Methods
Materials
Protein G-Sepharose and glutathione-Sepharose were purchased from Amersham Bioscience; [γ-^{32}P]ATP from PerkinElmer; thapsigargin, anti-FLAG M2-agarose, tetracycline, hygromycin B, Tween 20 and DMSO from Sigma; GFP-Trap from Chromotek; trypsin and Asp-N endoproteinase from Boehringer Mannheim; PD184352 and PD0325901 from Axon Medchem; FuGENE 6 transfection reagent and protease-inhibitor cocktail tablets from Roche; Flip-In T-REx HEK293 cells, zeocin, blasticidin, colloidal blue staining kit and pre-cast SDS polyacrylamide Bis-Tris gels from Invitrogen; Nonidet P40 from Fluka; and fura-2-acetoxymethyl ester (fura-2-AM) from Calbiochem. ORAI1–CFP vector was provided by Anjana Rao (Immune Disease Institute, Harvard University, Boston, MA) and distributed by Addgene (plasmid #12199).

Antibodies
The phospho-specific antibody that recognizes the phosphorylated forms of ERK1 and ERK2 was a rabbit monoclonal antibody; the antibody against total ERK1/2 was a rabbit polyclonal antibody; the antibody against phospho-MAPK/CDK substrate (PXpSP or pSPXR/K) was a rabbit monoclonal antibody. All these antibodies were from Cell Signaling Technologies. The rabbit polyclonal anti-ORAI1 antibody and the mouse monoclonal anti-GAPDH antibody were from Abcam. Mouse monoclonal anti-FLAG M2 antibody was from Sigma, and the rabbit polyclonal anti-STIM1 antibody from ProSci (Poway, CA).

General methods and solutions
Restriction enzyme digests, DNA ligations, and other recombinant DNA procedures were performed following standard protocols. All mutageneses were performed using the QuickChange site-directed mutagenesis method (Stratagene) with the KOD polymerase (Novagen). DNA constructs used for transfection were purified from *E. coli* DH5α using Qiagen Plasmid kits according to the manufacturer's protocol. All DNA constructs were verified by DNA sequencing, which was performed by the Sequencing Service (College of Life Sciences, University of Dundee, UK) using DYEnamic ET terminator chemistry (Amersham Biosciences) on Applied Biosystems automated DNA sequencers. The lysis buffer used for HEK293 cells was 50 mM Tris-HCl (pH 7.5), 1 mM EGTA, 1 mM EDTA, 1% (v/v) Nonidet P40 (substitute), 1 mM sodium orthovanadate, 50 mM sodium fluoride, 5 mM sodium pyrophosphate, 0.27 M sucrose, 0.1% (v/v) 2-mercaptoethanol, 1 mM benzamidine and 0.1 mM PMSF. Buffer A was 50 mM Tris-HCl (pH 7.5), 0.1 mM EGTA and 0.1% (v/v) 2-mercaptoethanol. SDS sample buffer contained 50 mM Tris-HCl (pH 6.8), 2% (w/v) SDS, 10% (v/v) glycerol, 0.005% (w/v) bromophenol blue and 1% (v/v) 2-mercaptoethanol. TBS-T buffer was Tris-HCl (pH 7.5), 0.15 M NaCl and 0.5% (v/v) Tween 20. All protein concentrations were determined using the Bradford reagent (Bio-Rad) and by measuring the absorbance at 595 nm.

Expression and purification of GST–STIM1 [235-END] in *E. coli*

The cytosolic domain of STIM1 (bases 235-END) was cloned into pGEX-6P vector, and used to transform BL21 *E. coli* cells. Cultures (0.5 l) were grown at 37°C in Luria Broth containing 100 µg/ml ampicillin until the absorbance at 600 nm was 0.6–0.8. Isopropyl β-D-thiogalactopyranoside (30 µM) was then added and the cells were cultured for a further 16 hours at 26°C. Cells were isolated by centrifugation, resuspended in 30 ml of ice-cold lysis buffer, and lysed in one round of freeze/thawing, followed by sonication (Branson Digital Sonifier; ten 15-second pulses with a setting of 45% amplitude) to fragment DNA. Lysates were centrifuged at 4°C for 15 minutes at 26,000 *g*. The GST fusion protein was affinity-purified on 0.25 ml glutathione-Sepharose and eluted in buffer A containing 0.27 M sucrose and 20 mM glutathione.

In vitro kinase assays

Protein kinases ERK1 and ERK2 were expressed in *E. coli*. Both kinases were of human origin and encoded full-length proteins. The procedures for expressing the protein kinases used in the present study have been detailed previously (Bain et al., 2003; Davies et al., 2000).

All assays (25 µl volume) were carried out at 30°C and for 15 minutes. The concentration of magnesium acetate in the assays was 10 mM, and [γ-^{32}P]ATP (~300 cpm/pmol) was used at 100 µM. The assays were initiated with Mg-ATP. Positive controls of kinase assays were performed with myelin basic protein (MBP, 0.33 mg/ml). The samples were subjected to electrophoresis on a Bis-Tris 10% polyacrylamide gel, which was stained with colloidal blue and then autoradiographed. Other experimental conditions were as described (Bain et al., 2003; Bain et al., 2007).

Mapping the sites on STIM1 that are phosphorylated by ERK1/2

GST–STIM1$^{235-END}$ (5 µg) purified from *E. coli* was incubated with active ERK1 or ERK2 (0.1 µg), also purified from *E. coli*, at 30°C for 15 minutes in buffer A containing 10 mM MgCl$_2$, 5–50 µM ATP in a total reaction volume of 25 µl. The reaction was terminated by addition of LDS sample buffer. Dithiothreitol (DTT) was added to a final concentration of 10 mM, the samples heated at 95°C for 4 minutes and cooled for 10 minutes at room temperature. Iodoacetamide was then added to a final concentration of 50 mM and the samples left in the dark for 30 minutes at room temperature to alkylate the cysteine residues. The samples were subjected to electrophoresis on a Bis-Tris 10% polyacrylamide gel and stained with colloidal blue. Then, the GST–STIM1$^{235-END}$ bands were excised, cut into smaller pieces and washed sequentially for 10 minutes on a vibrating platform with 1 ml of each of the following: water, a 1:1 (v/v) mixture of water and acetonitrile, 0.1 M ammonium bicarbonate, a 1:1 (v/v) mixture of 0.1 M ammonium bicarbonate and acetonitrile, and finally acetonitrile. The gel pieces were dried and then rehydrated in 25 mM triethylammonium bicarbonate containing 5 µg/ml of MS-grade trypsin or Asp-N protease. After 16 hours at 30°C, an equal volume of acetonitrile was added, and the mixture was incubated on a shaking platform for 10 minutes. The supernatant was dried, and a further extraction with 0.1 ml of 50% acetonitrile and 2.5% formic acid was performed.

After proteolysis, samples were analysed by one or more MS methods: first, by LC-MS with precursor 79 scanning on an Applied Biosystems 4000 Q-Trap system coupled to a Dionex Ultimate/Switchos/Famos LC (Williamson et al., 2006); and second, by LC-MS on a Thermo-Electron LTQ-Orbitrap mass spectrometer coupled to a Dionex Ultimate 3000 nanoliquid chromatography system. Data files were searched using Mascot (www.matrixscience.com) run on an in-house system containing the tagged STIM1 sequence, with the following parameters: Q-Trap analyses with a ±1.2 Da peptide mass tolerance [#13C=1] and ±0.6 Da fragment mass tolerance allowing for carbamidomethyl (C) as a fixed modification and for oxidation (M) and phospho (ST) as variable modifications. Individual MS/MS spectra were inspected using Analyst software where necessary. OrbiTrap analyses with a ±20 ppm peptide mass tolerance [#13C=1] and ±0.8 Da fragment mass tolerance allowing for carbamidomethyl (C) as a fixed modification and for oxidation (M), phospho (ST) and phospho (Y) as variable modifications. The individual MS/MS spectra were inspected using Xcalibur 2.2 software where necessary. Unless noted otherwise, all peptides were identified with individual ion scores indicating identity or extensive homology ($P<0.05$).

HEK293 culture and generation of stable cell lines

Mouse Stim1 (accession number NM_009287) was cloned as a *Bam*HI-*Not*I into pcDNA5/FRT/TO vector (Invitrogen) carrying an N-terminal FLAG or C-terminal GFP tag. To generate Flip-In T-REx HEK293 cells (Invitrogen) able to inducibly express tagged STIM1, the cells were transfected with a mixture containing the cDNA in pcDNA5/FRT/TO vector and the pOG44 vector (1:9) using polyethylenimine. After 48 hours, the medium was changed to medium supplemented with 100 µg/ml hygromycin B plus 15 µg/ml blasticidin to select stably transfected cells. Resistant cell lines were screened for FLAG or GFP expression by western blotting. Flip-In T-REx HEK293 cells were cultured on 10-cm diameter dishes in Dulbecco's modified Eagle's medium (DMEM) with 10% (v/v) fetal bovine serum, 2 mM L-glutamine, 100 U/ml penicillin, 0.1 mg/ml streptomycin, 100 µg/ml hygromycin B, and 15 µg/ml blasticidin in a humidified atmosphere of air and CO$_2$ at 37°C.

Cells were treated with 1 µg/ml tetracycline for 12–16 hours in serum-free culture medium before assay to induce expression of tagged STIM1. All the experiments shown in this work were performed after 14–16 hours of serum deprivation.

FLAG-tagged proteins were purified from samples by incubating 20 µl of FLAG–agarose beads with 4 mg of the clarified lysates for 2 hours at 4°C. Clarification was performed after lysis with 1 ml of ice-cold lysis buffer per dish and centrifugation at 4°C for 15 minutes at 26,000 *g*. The immunoprecipitates were washed four times with 1 ml lysis buffer containing 0.5 M NaCl and twice with 1 ml of buffer A. In the co-immunoprecipitation assay, FLAG–beads were washed three times with lysis buffer containing 0.15 M NaCl and twice with buffer A. Proteins were eluted from the FLAG–beads by the addition of 25 µl NuPAGE-LDS sample buffer to the beads. Eluted proteins were reduced by the addition of 10 mM DTT followed by heating at 95°C for 4 minutes.

Mapping in vivo phosphorylation sites in STIM1–GFP expressed in HEK293 cells

HEK293 cells expressing STIM1–GFP were treated with 1 µM thapsigargin for 10 minutes in Ca^{2+}-free Hank's balanced salt solution (HBSS, Invitrogen) or with 400 ng/ml TPA for 15 minutes in Ca^{2+}-containing HBSS. The treated cells were lysed with 0.5 ml of ice-cold lysis buffer per dish and the lysates clarified by centrifugation at 4°C for 15 minutes at 26,000 *g*. STIM1–GFP was purified from control, thapsigargin-treated samples or TPA-treated samples by incubation with GFP–Trap as described in the literature (Trinkle-Mulcahy et al., 2008). Briefly, equilibrated GFP–Trap beads (30 µl) were added to the cell lysates (4 mg) and incubated with gentle mixing for 1 hour at 4°C. The beads were washed twice with 1 ml lysis buffer containing 0.5 M NaCl and once with 1 ml buffer A. Proteins were eluted from the GFP–Trap beads by the addition of 25 µl NuPAGE-LDS sample buffer to the beads. Eluted proteins were reduced by the addition of 10 mM DTT followed by heating at 95°C for 4 minutes. The samples were then alkylated by the addition of 50 mM iodoacetamide followed by incubation in the dark for 30 minutes at room temperature. Samples were then electrophoresed on a 4–12% polyacrylamide gel, which was stained with colloidal blue. The STIM1–GFP was excised from the gel, cut into smaller pieces and washed as described above. For the identification of phosphorylation sites, the Asp-N proteolytic digests were analyzed by LC-MS as described above.

Cytosolic free calcium concentration measurement

Cytosolic free calcium concentration, [Ca^{2+}]$_i$, was measured basically as described elsewhere (Gomez-Fernandez et al., 2009; Gutierrez-Martin et al., 2005; Martin-Romero et al., 2008). Briefly, HEK293 cells were plated on poly-L-lysine-coated glass coverslips and after 2 days of culture they were loaded with fura-2-AM in serum-free medium for 60 minutes with 2 µM fura-2-AM plus 0.025% Pluronic-F127, and rinsed thoroughly with HBSS containing Ca^{2+} and Mg^{2+}. [Ca^{2+}]$_i$ was measured with an inverted microscope Nikon TE2000-U equipped with microincubation platform DH-40i (Warner Instruments, Hamden, CT). Ratio fluorescence images were obtained with excitation filters of 340 and 380 nm, a 510 nm dichroic mirror, and a 520 nm emission filter (Semrock, Rochester, NY). Digital images were taken with a Hamamatsu C9100-02 electron multiplier CCD camera. All measurements were performed at 37°C (heater controller TC-324B from Warner Instruments).

Depletion of Ca^{2+}-stores was triggered by incubating cells with 1 µM thapsigargin in Ca^{2+}-free HBSS with the following composition: 138 mM NaCl, 5.3 mM KCl, 0.34 mM Na$_2$HPO$_4$, 0.44 mM KH$_2$PO$_4$, 4.17 mM NaHCO$_3$, 4 mM Mg^{2+} and 0.1 mM EGTA (pH 7.4). SOCE was measured by monitoring the increase in [Ca^{2+}]$_i$ after the addition of 2 mM CaCl$_2$ to the thapsigargin-containing medium.

Wide-field fluorescence microscopy, TIRF and FRET analysis

Wide-field microscopy and TIRF (total internal reflection fluorescence) experiments were performed at the Microscopy Facility of the College of Life Sciences, University of Dundee, UK. For wide-field fluorescence microscopy, HEK293 cells expressing STIM1–GFP were treated in Ca^{2+}-free HBSS. Then, cells were fixed in freshly made 4% paraformaldehyde and mounted in Hydromount. Images of fixed cells were taken on a DeltaVision Widefield microscope with a 60× NA 1.45 oil immersion objective, followed by iterative deconvolution.

Similarly, for TIRF experiments, HEK293 cells expressing STIM1–GFP were treated with 1 µM thapsigargin in Ca^{2+}-free HBSS as indicated for [Ca^{2+}]$_i$ measurements. These experiments were performed at 37°C on an inverted microscope (Nikon TIRF imaging system) that was equipped with an environmental chamber. Images were taken with a Plan Apo 60× NA 1.45 oil immersion objective and recorded with an intensified EM-CCD camera (Hamamatsu).

FRET experiments were performed at the Cytomics Unit of Core Facility Services of the University of Extremadura, Badajoz, Spain. Eight hours after plating, STIM1–GFP cells were transfected with ORAI1–CFP vector as described (Prakriya et al., 2006). STIM1–GFP expression was induced 24 hours later with tetracycline as indicated above. FRET analysis was performed with Fluoview 1000 confocal microscope (Olympus, Hamburg, Germany), using FV10-ASW software (Olympus) equipped with FRET module and environmental chamber. A water immersion 60× NA 1.2 objective was used. Controls with CFP or GFP only were used to set up the system. All analyses were done under the same conditions. Acquisition was done following software instructions of the Donor Photobleaching Method (Olympus). FRET quantification was performed measuring PM areas only.

Supplementary material available online at
http://jcs.biologists.org/cgi/content/full/123/18/3084/DC1

References

Ambudkar, I. S., Ong, H. L., Liu, X., Bandyopadhyay, B. and Cheng, K. T. (2007). TRPC1: the link between functionally distinct store-operated calcium channels. *Cell Calcium* **42**, 213-223.

Bain, J., McLauchlan, H., Elliott, M. and Cohen, P. (2003). The specificities of protein kinase inhibitors: an update. *Biochem. J.* **371**, 199-204.

Bain, J., Plater, L., Elliott, M., Shpiro, N., Hastie, C. J., McLauchlan, H., Klevernic, I., Arthur, J. S., Alessi, D. R. and Cohen, P. (2007). The selectivity of protein kinase inhibitors: a further update. *Biochem. J.* **408**, 297-315.

Cahalan, M. D. (2009). STIMulating store-operated Ca(2+) entry. *Nat. Cell Biol.* **11**, 669-677.

Davies, S. P., Reddy, H., Caivano, M. and Cohen, P. (2000). Specificity and mechanism of action of some commonly used protein kinase inhibitors. *Biochem. J.* **351**, 95-105.

Feske, S., Gwack, Y., Prakriya, M., Srikanth, S., Puppel, S. H., Tanasa, B., Hogan, P. G., Lewis, R. S., Daly, M. and Rao, A. (2006). A mutation in Orai1 causes immune deficiency by abrogating CRAC channel function. *Nature* **441**, 179-185.

Gomez-Fernandez, C., Pozo-Guisado, E., Ganan-Parra, M., Perianes, M. J., Alvarez, I. S. and Martin-Romero, F. J. (2009). Relocalization of STIM1 in mouse oocytes at fertilization: early involvement of store-operated calcium entry. *Reproduction* **138**, 211-221.

Gutierrez-Martin, Y., Martin-Romero, F. J. and Henao, F. (2005). Store-operated calcium entry in differentiated C2C12 skeletal muscle cells. *Biochim. Biophys. Acta* **1711**, 33-40.

Liou, J., Kim, M. L., Heo, W. D., Jones, J. T., Myers, J. W., Ferrell, J. E., Jr and Meyer, T. (2005). STIM is a Ca(2+) sensor essential for Ca(2+)-store-depletion-triggered Ca(2+) influx. *Curr. Biol.* **15**, 1235-1241.

Liou, J., Fivaz, M., Inoue, T. and Meyer, T. (2007). Live-cell imaging reveals sequential oligomerization and local plasma membrane targeting of stromal interaction molecule 1 after Ca2+ store depletion. *Proc. Natl. Acad. Sci. USA* **104**, 9301-9306.

Manji, S. S., Parker, N. J., Williams, R. T., van Stekelenburg, L., Pearson, R. B., Dziadek, M. and Smith, P. J. (2000). STIM1: a novel phosphoprotein located at the cell surface. *Biochim. Biophys. Acta* **1481**, 147-155.

Martin-Romero, F. J., Ortiz-de-Galisteo, J. R., Lara-Laranjeira, J., Dominguez-Arroyo, J. A., Gonzalez-Carrera, E. and Alvarez, I. S. (2008). Store-operated calcium entry in human oocytes and sensitivity to oxidative stress. *Biol. Reprod.* **78**, 307-315.

Muik, M., Frischauf, I., Derler, I., Fahrner, M., Bergsmann, J., Eder, P., Schindl, R., Hesch, C., Polzinger, B., Fritsch, R. et al. (2008). Dynamic coupling of the putative coiled-coil domain of ORAI1 with STIM1 mediates ORAI1 channel activation. *J. Biol. Chem.* **283**, 8014-8022.

Olsen, J. V., Blagoev, B., Gnad, F., Macek, B., Kumar, C., Mortensen, P. and Mann, M. (2006). Global, in vivo, and site-specific phosphorylation dynamics in signaling networks. *Cell* **127**, 635-648.

Park, C. Y., Hoover, P. J., Mullins, F. M., Bachhawat, P., Covington, E. D., Raunser, S., Walz, T., Garcia, K. C., Dolmetsch, R. E. and Lewis, R. S. (2009). STIM1 clusters and activates CRAC channels via direct binding of a cytosolic domain to Orai1. *Cell* **136**, 876-890.

Prakriya, M., Feske, S., Gwack, Y., Srikanth, S., Rao, A. and Hogan, P. G. (2006). Orai1 is an essential pore subunit of the CRAC channel. *Nature* **443**, 230-233.

Roos, J., DiGregorio, P. J., Yeromin, A. V., Ohlsen, K., Lioudyno, M., Zhang, S., Safrina, O., Kozak, J. A., Wagner, S. L., Cahalan, M. D. et al. (2005). STIM1, an essential and conserved component of store-operated Ca(2+) channel function. *J. Cell Biol.* **169**, 435-445.

Rosado, J. A. and Sage, S. O. (2001). Role of the ERK pathway in the activation of store-mediated calcium entry in human platelets. *J. Biol. Chem.* **276**, 15659-15665.

Rubinfeld, H. and Seger, R. (2005). The ERK cascade: a prototype of MAPK signaling. *Mol. Biotechnol.* **31**, 151-174.

Smyth, J. T., DeHaven, W. I., Bird, G. S. and Putney, J. W., Jr (2007). Role of the microtubule cytoskeleton in the function of the store-operated Ca2+ channel activator STIM1. *J. Cell Sci.* **120**, 3762-3771.

Smyth, J. T., DeHaven, W. I., Bird, G. S. and Putney, J. W., Jr (2008). Ca2+-store-dependent and -independent reversal of Stim1 localization and function. *J. Cell Sci.* **121**, 762-772.

Smyth, J. T., Petranka, J. G., Boyles, R. R., Dehaven, W. I., Fukushima, M., Johnson, K. L., Williams, J. G. and Putney, Jr, J. W. (2009). Phosphorylation of STIM1 underlies suppression of store-operated calcium entry during mitosis. *Nat. Cell Biol.* **11**, 1465-1472.

Soboloff, J., Spassova, M. A., Tang, X. D., Hewavitharana, T., Xu, W. and Gill, D. L. (2006). Orai1 and STIM reconstitute store-operated calcium channel function. *J. Biol. Chem.* **281**, 20661-20665.

Srikanth, S., Jung, H. J., Kim, K. D., Souda, P., Whitelegge, J. and Gwack, Y. (2010). A novel EF-hand protein, CRACR2A, is a cytosolic Ca2+ sensor that stabilizes CRAC channels in T cells. *Nat. Cell. Biol.* **12**, 436-446.

Trinkle-Mulcahy, L., Boulon, S., Lam, Y. W., Urcia, R., Boisvert, F. M., Vandermoere, F., Morrice, N. A., Swift, S., Rothbauer, U., Leonhardt, H. et al. (2008). Identifying specific protein interaction partners using quantitative mass spectrometry and bead proteomes. *J. Cell Biol.* **183**, 223-239.

Vig, M., Peinelt, C., Beck, A., Koomoa, D. L., Rabah, D., Koblan-Huberson, M., Kraft, S., Turner, H., Fleig, A., Penner, R. et al. (2006). CRACM1 is a plasma membrane protein essential for store-operated Ca(2+) entry. *Science* **312**, 1220-1223.

Williamson, B. L., Marchese, J. and Morrice, N. A. (2006). Automated identification and quantification of protein phosphorylation sites by LC/MS on a hybrid triple quadrupole linear ion trap mass spectrometer. *Mol. Cell Proteomics* **5**, 337-346.

Yeromin, A. V., Zhang, S. L., Jiang, W., Yu, Y., Safrina, O. and Cahalan, M. D. (2006). Molecular identification of the CRAC channel by altered ion selectivity in a mutant of Orai. *Nature* **443**, 226-229.

Yu, F., Sun, L. and Machaca, K. (2009). Orai1 internalization and STIM1 clustering inhibition modulate SOCE inactivation during meiosis. *Proc. Natl. Acad. Sci. USA* **106**, 17401-17406.

Yuan, J. P., Zeng, W., Huang, G. N., Worley, P. F. and Muallem, S. (2007). STIM1 heteromultimerizes TRPC channels to determine their function as store-operated channels. *Nat. Cell Biol.* **9**, 636-645.

Yuan, J. P., Zeng, W., Dorwart, M. R., Choi, Y. J., Worley, P. F. and Muallem, S. (2009). SOAR and the polybasic STIM1 domains gate and regulate Orai channels. *Nat. Cell Biol.* **11**, 337-343.

Zeng, W., Yuan, J. P., Kim, M. S., Choi, Y. J., Huang, G. N., Worley, P. F. and Muallem, S. (2008). STIM1 gates TRPC channels, but not Orai1, by electrostatic interaction. *Mol. Cell* **32**, 439-448.

Zhang, S. L., Yeromin, A. V., Zhang, X. H., Yu, Y., Safrina, O., Penna, A., Roos, J., Stauderman, K. A. and Cahalan, M. D. (2006). Genome-wide RNAi screen of Ca(2+) influx identifies genes that regulate Ca(2+) release-activated Ca(2+) channel activity. *Proc. Natl. Acad. Sci. USA* **103**, 9357-9362.